3-D Shape Reconstruction of Pipe with Omni-Directional Laser and Omni-Directional Camera

Kenki Matsui, Atsushi Yamashita and Toru Kaneko

E-mail: {f0930058, tayamas, tmtkane} @ipc.shizuoka.ac.jp, TEL: +81-53-478-1067, FAX: +81-53-478-1067

KEYWORDS : Omni-Directional Camera , Omni-Directional Laser, Pipe Inspection

A lot of plumbings such as gas pipes and water pipes exist in factories and so on. It is difficult for humans to inspect them directly because they are laid underground. Therefore, automated inspection by robots which equipped with ca mera is desirable, and great efforts have been done to solve this problem. However, many of existing inspection robots have to rotate the camera to record images in piping because a conventional camera with narrow view can see only one direction while piping has a cylindrical geometry. The use of an omni-directional camera that can take images of 360° in surroundings at a time is effective for the solution of such problem. Though, the shape measurement is difficult only with the omni-directional camera. Then, in this paper, we propose a reconstruction method of piping shape by using an omni-directional camera and an omni-directional laser with a light section method and a structure from motion. The validity of the proposed method is shown through experiments.

Manuscript received: July 15, 2009 / Accepted: August 15, 2009

1. INTRODUCTION

A lot of plumbings such as gas pipes and water pipes exist in factories, and so on. These facilities are important and indispensable for our living.

However, these pipes become deteriorated by ageing and internal damage comes to existence. If the damage grows large, a serious accident might happen.

To find such damage at the early stage, and to take precautions against possible accidents, it is important to recognize the pipe state. However it is difficult for humans to inspect the pipe state directly because they are laid underground. Therefore, automated inspection by robots which equipped with camera is desirable and many efforts have been done to solve such problem [1][2][3][4][5][6].

However, many of existing inspection robots have to rotate the camera to record images in piping because a conventional camera with narrow view can see only one direction while piping has a cylindrical geometry. There is a problem that inspection robot have to stop every time at the point where the robot records the image. Therefore, it takes long time to measure pipe shape.

On the other hand, omni-directional vision sensors with a widefield of view have been invented; e.g. a fisheye camera and an omni-directional camera. They have a variety of potential applications, such as mobile robot navigation [7], and telepresense technology [8]. Particularly, previous studies showed that an omni-directional camera is effective in measurement and recognition of environment [9].

Kannala et al. proposed a pipe inspection method using omni-directional vision sensor for robot vision [10]. The use of the omni-directional vision sensor that can take images of 360° in surrounding at a time is effective for pipe inspection.

Kannala et al. use the structure from motion technique which is a kind of passive measurement. However, the method has to extract and track feature points to get corresponding between images. If corresponding point acquisition fails, the measurement accuracy is decreases.

To solve this problem, a light section method which is a kind of active measurement is proposed instead of passive measurement like the structure from motion. Light section method has an advantage that the method uses only single image for measurement and need not to get corresponding points. Therefore, measurement accuracy is more precisely than structure from motion and the method uses various fields [11][12].

However, in general, the light section method requires that the position and the orientation of the camera be constant while measurement. Therefore, if the camera moves, it is difficult to integrate of the measurement results.

On the other hand, structure from motion technique has the advantage that can estimate the camera motion (the relative relations of camera positions and orientations) with 3-D measurement.

Then in this paper, we propose a 3-D measurement method by using an omni-directional camera and an omni-directional laser with light section method and structure from motion. Our method calculates 3-D coordinates by light section method. Then, By Integrating the 3-D coordinate with information of camera motion estimated by structure from motion technique, the shape of the pipe is reconstructed.

2. OUTLINE

An inspection robot executes 3-D measurement by using an omni-directional camera (Fig.1) and a laser source that can emit laser light in all direction (Fig.2).

The process of our method is shown in Fig.3. As the first step, the inspection robot acquires an omni-directional image sequence during its locomotion while emitting laser light.

The second step calculates 3-D coordinates of measurement points by light section method.

The third step estimates a camera motion by structure from motion method and integrates measurement results.

By repeating the above-mentioned procedure, the shape of pipe is reconstructed.

Fig.1 Omni-directional camera

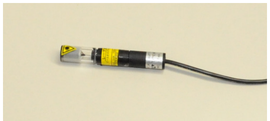

Fig.2 Omni-directional laser

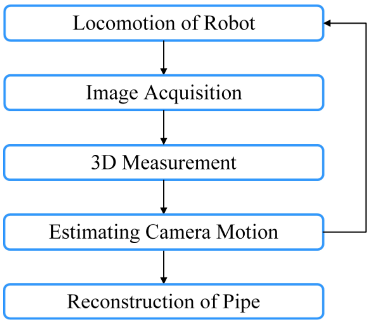

Fig.3 Process

3. 3-D MEASUREMNT

We use light the section method for 3-D measurement.

First, we extract image coordinates of laser light from an omni-directional image sequence.

Then, the 3-D coordinates of measurement point are given as the cross-point of a ray vector and the laser light.

3.1 LASER LIGHT EXTRACTION

The laser light reflected from the measurement object is captured by the omni-directional camera as an area with some width. Therefore, we have to extract a peak (the pixel that has highest intensity) from the area that can be considered to be the laser light on image. We use the Gaussian approximation method [13] to extract the peak.

In order to detect the laser light, we scan radially from the center of the omni-directional image (Fig.4). We approximate the changing of intensity value in the radial direction to Gaussian distribution (Fig.5).

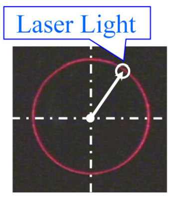

Fig.4 Radial scanning

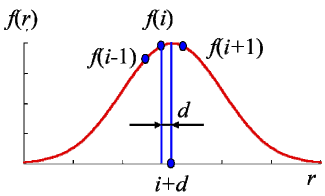

Fig.5 Gaussian distribution

Then, we select three highest intensity values from the laser light. The subpixel offset d is calculated from these values by Eq.(1).

$$d = \frac{1}{2}\frac{\ln(f(i-1)) - \ln(f(i+1))}{\ln(f(i-1)) - 2\ln(f(i)) + \ln(f(i+1))} \tag{1}$$

where $f(i)$ means intensity value at i which is an image coordinate of the observed peak intensity.

As a result, $(i + d)$ is obtained as the image coordinate of the laser light.

3.2 3-D COORDINATES CALCULATION

We define a unit vector which starts at the center of projection and ends at a measurement point in 3D space as a ray vector $\mathbf{r} = [x, y, z]^T$, where T stands for transposition of vector matrix.

The omni-directional camera has a hyperboloid mirror in front of lens of a conventional camera. Therefore, as shown in Fig.6, ray vector $\mathbf{r}$ is directed from the focus of the hyperboloid mirror to the reflection point of the ray on the mirror surface.

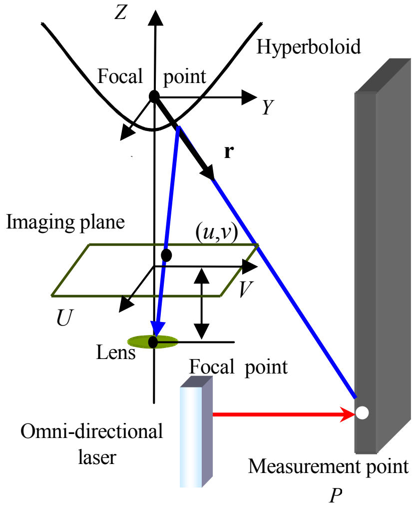

Fig.6 Calculation of 3-D coordinates

Ray vector $\mathbf{r}$ is calculated from image coordinates $[u, v]^T$ of the laser light using Eqs.(2), (3) and (4). In these equations, a, b are the hyperboloid parameters, and f is the image distance (the distance between the center of the lens and the image plane) of camera.

$$\mathbf{r} = \lambda \begin{bmatrix} su \\ sv \\ sf - 2c \end{bmatrix} \tag{2}$$

$$s = \frac{a^2\left(f\sqrt{a^2+b^2} + b\sqrt{u^2+v^2+f^2}\right)}{a^2 f^2 - b^2(u^2+v^2)} \tag{3}$$

$$c = \sqrt{a^2+b^2} \tag{4}$$

Then, we define the plane of laser light as Eq.(5). In the equation, k_1, k_2, k_3, k_4 are the planar parameters, and there are calibrated in advance.

$$k_1 x + k_2 y + k_3 z + k_4 = 0 \tag{5}$$

From Eqs.(2), (3), (4) and (5) the 3-D coordinates of measurement point is calculated by Eq.(6).

$$\begin{bmatrix} x_p \\ y_p \\ z_p \end{bmatrix} = \frac{-k_4}{k_1 su + k_2 sv + k_3(sf - 2c)} \begin{bmatrix} su \\ sv \\ sf - 2c \end{bmatrix} \tag{6}$$

4. CAMERA MOTION ESTIMATION

We use a structure from motion technique for camera motion estimation [14].

First, the robot acquires an omni-directional image sequence during its locomotion.

Second, the method extracts and tracks feature points to get corresponding points in the omni-directional image sequence.

The camera motion is estimated by the linear estimation, which uses the positions of corresponding points in two images taken at each observation point.

In order to estimate the camera motion more precisely, re-estimation of camera motion is performed with the nonlinear estimation.

4.1 CORRESPONDING POINT ACQUISITION

For getting corresponding points between images in the omni-directional image sequence, the method extracts feature points in the first image and then tracks them along the sequence. In our method, we use SIFT (Scale Invariant Feature Transform) algorithm [15].

First, we extract feature points. By comparing these points between two images taken before and after the robot movement, we get corresponding points which are regarded as the same point in 3-D space (Fig.7).

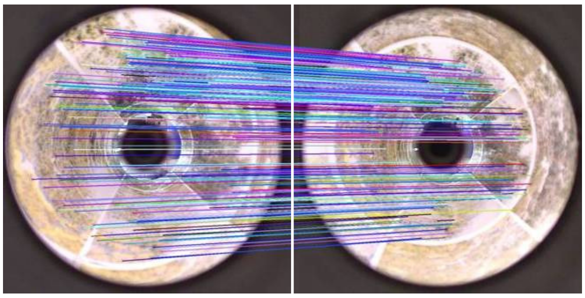

(a) Image acquired before robot movement (b) Image acquired after robot movement

Fig.7 Corresponding point acquisition

4.2 OUTLIER REJECTION

All feature points tracked along the image sequence do not behave as corresponding points because of image noise and so on. Feature points of mistracking should be rejected as outliers. To solve this problem, we employ a method of RANSAC (RANdom SAmple Consensus) [16].

4.3 ESTIMATION OF CAMERA MOTION

In order to estimate camera motion, we calculate the essential matrix which contains information about relative position and orientation differences between two observation points.

Essential Matrix $\mathbf{E}$ satisfies Eq.(7).

$$\mathbf{r}_i'^T \mathbf{E} \mathbf{r}_i = 0 \tag{7}$$

where $\mathbf{r} = [x_i, y_i, z_i]^T$, $\mathbf{r}' = [x'_i, y'_i, z'_i]^T$ are the ray vectors of the correcting point in two images, respectively. Equation (7) is transformed into Eq.(8).

$$\mathbf{u}_i^T \mathbf{e} = 0 \tag{8}$$

where

$\mathbf{u}_i=[x_ix'_i, y_ix'_i, z_ix'_i, x_iy'_i, y_iy'_i, z_iy'_i, x_iz'_i, y_iz'_i, z_iz'_i]^T$

$\mathbf{e}=[e_{11}, e_{12}, e_{13}, e_{21}, e_{22}, e_{23}, e_{31}, e_{32}, e_{33}]^T$

Essential matrix $\mathbf{E}$ is obtained by solving simultaneous equation for more than eight pairs of corresponding rays vectors. This means that we solve Eq.(9).

$$\min_{e} \|\mathbf{U}\mathbf{e}\|^2 \tag{9}$$

where $\mathbf{U} = [\mathbf{u}_1, \mathbf{u}_2, \cdots, \mathbf{u}_n]^T$. Essential matrix $\mathbf{E}$ is obtained from $\mathbf{e}$ which is given as the eigenvector of the smallest eigenvalue of $\mathbf{U}^T\mathbf{U}$.

From the essential matrix $\mathbf{E}$, we calculate rotation matrix $\mathbf{R}$ and translation vector $\mathbf{t}$.

Essential matrix $\mathbf{E}$ is represented by rotation matrix $\mathbf{R}$ and translation vector $\mathbf{t} = [t_x, t_y, t_z]^T$.

$$\mathbf{E} = \mathbf{R}\mathbf{T} \tag{10}$$

Here, $\mathbf{T}$ is a matrix given as follows.

$$\mathbf{T} = \begin{bmatrix} 0 & -t_z & t_y \\ t_z & 0 & -t_x \\ -t_y & t_x & 0 \end{bmatrix} \tag{11}$$

We calculate $\mathbf{R}$ and $\mathbf{T}$ from essential matrix $\mathbf{E}$ by singular valve decomposition.

4.4 RE-ESTIMATION OF CAMERA MOTION

The Rotation matrix and translation vector estimated in Section 4.3 may not be always good results because the results do not consider the various errors in images. Then, we re-estimate the camera motion in consideration of the measurement errors in each feature point.

We use bundle adjustment [17] for re-estimation of the camera motion. The method minimizes the sum of feature reprojection errors which means difference between the image coordinates of the original feature point and the reprojected coordinates of 3-D space.

4.5 SCALE MATCH METHOD

The structure from motion technique cannot determine the distance $|\mathbf{t}|$ between two observation points because the measurement only uses images for input and does not get any scale information.

However, the 3-D coordinate of point which measured by light section method includes scale information. Therefore, we use the measurement result by light section method for scale matching.

First, we measure the 3-D coordinates of a point by light section method. Then, we measure the 3-D coordinates of the same point by structure from motion technique (the green circle in Fig.8).

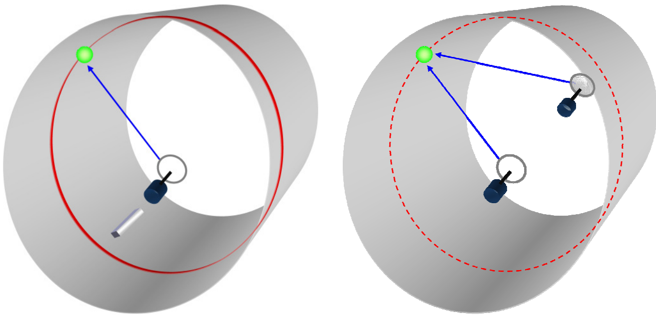

(a) Measurement by light section method (b) Measurement by structure from motion

Fig.8 Scale matching

Scale matching is realized by making the 3-D coordinates of the same point as close as possible. Minimization of deviation of the two resultant coordinates of the same point is more sensitive when the point lies farther from the observation point. Therefore it is appropriate to minimize the distances of coordinates. Scale s' is calculated by Eq.(12).

$$\min \sum_{k=1}^{m} \|\log(\mathbf{p}_k) - \log(s'\mathbf{p}_k)\|^2 \tag{12}$$

where $\mathbf{p}_k = [x_k, y_k, z_k]^T$ represents measurement result by light section method, and $\mathbf{p}_k' = [x_k', y_k', z_k']^T$ represents measurement result by structure from motion technique, respectively.

5. EXPERIMENT

In the experiment we measured two objects. The one is a rectangular container and another is a pipe. The size of input image sequence is 1920 × 1080 pixels.

In the 3-D measurement, we use image without ambient illumination. Also, in the camera motion estimation, we use image with ambient illumination.

5.1 ACCURACY EVALUATION EXPERIMENT

The experimental environment is shown in Fig.9.

We fix an omni-directional camera and an omni-directional laser to a jig (Fig.10). The laser light is emitting while lifting the jig in container. Then, we acquired an image sequence by using the omni-directional camera.

Figures 11 and 12 show acquired images with ambient illumination and without ambient illumination. Figure 13 shows the result of measurement. The result shows our proposed method can reconstruct the 3-D shape of container.

Table 1 shows the standard deviations from the least square planes. Table 2 shows angles between two planes calculated by least square method and Table 3 shows the distances between corner points.

The error of distance between corner points is within the theoretical value of our proposed method.

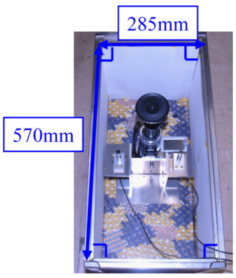

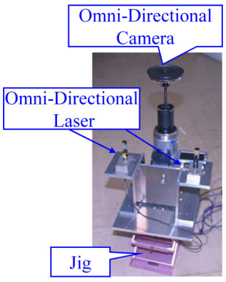

Fig.9 Experimental environment 1 Fig.10 Measurement device 1

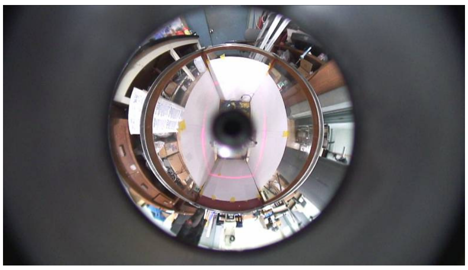

Fig.11 Image with ambient illumination 1

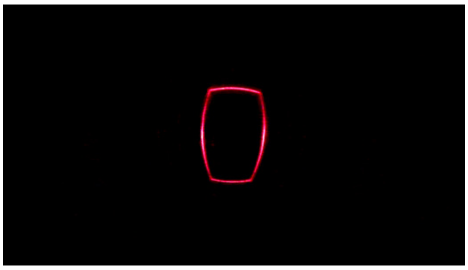

Fig.12 Image without ambient illumination 1

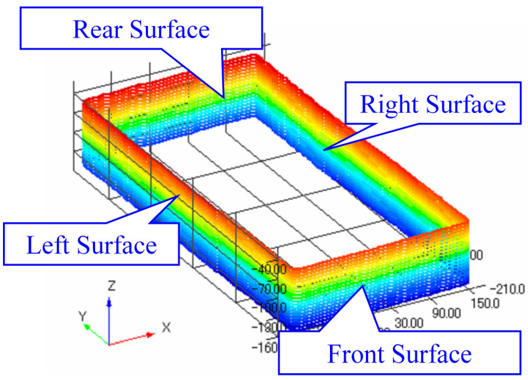

Fig.13 Reconstruct of container

Table 1 Standard deviations from the least square error plane

	Measurement value
Front Surface	1.08mm
Rear Surface	0.88mm
Left Surface	0.85mm
Right Surface	0.69mm

Table 2 Angles between two least square error planes

	Measurement value	True value
Front Surface and Left Surface	90.4deg	90.0deg
Rear Surface and Left Surface	89.6deg	90.0deg
Front Surface and Right Surface	90.6deg	90.0deg
Rear Surface and Right Surface	89.4deg	90.0deg

Table 3 Distances between corner points

	Measurement value	True value
Front Surface	282mm	285mm
Rear Surface	283mm	285mm
Left Surface	567mm	570mm
Right Surface	568mm	570mm

5.2 MEASUREMENT EXPERIMENT

Assuming pipe inspection, we prepare a pipe as a measurement object. The experimental environment is shown in Fig.14.

We install an omni-directional camera and an omni-directional laser to manipulator (Fig.15). The laser light is emitting while the manipulator moves in the pipe. Then, we acquired an image sequence by using the omni-directional camera.

Figures 16 and 17 show acquired images with ambient illumination and without ambient illumination. Figures 18 and 19 show the reconstruction result of pipe shape with our proposed method and the reconstruction result using movement information of manipulator, respectively. By comparing Figs.18 to 19, we can recognize our proposed method can reconstruct of the pipe shape with high precision.

Table 4 shows comparison of ground truth value and the measurement data. We compared inside diameter with the least square error circle which is calculated by measurement data. Also, we evaluate distance of manipulator measured by our proposed method. The error of inside diameter is within the theoretical value of our proposed method.

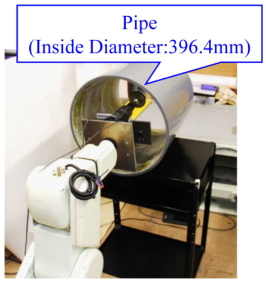

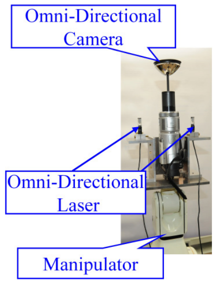

Fig.14 Experimental environment 2 Fig.15 Measurement device 2

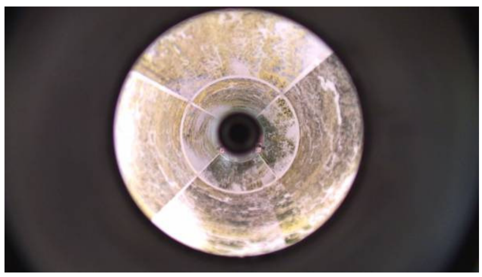

Fig.16 Image with ambient illumination 2

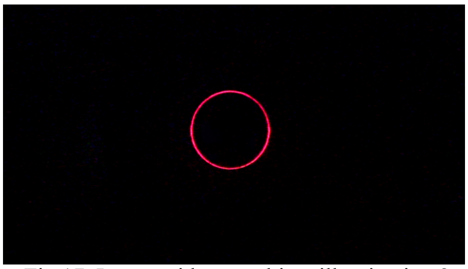

Fig.17 Image without ambient illumination 2

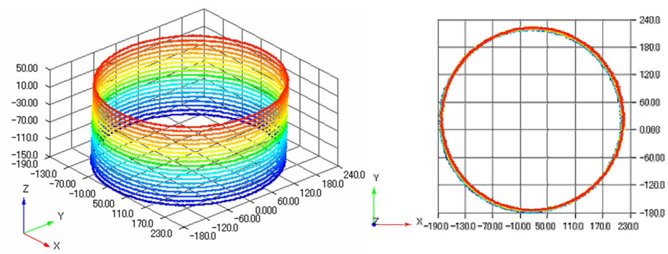

(a) Bird's-eye view (b) top view

Fig.18 Reconstruct of pipe shape with our proposed method

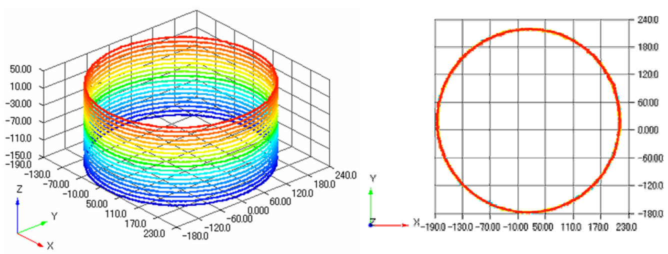

(a) Bird's-eye view (b) top view

Fig.19 Reconstruct of pipe shape with movement information of manipulator

Table 4 Accuracy evaluation

	Measurement value	Ground truth
Inside Diameter	394.6mm	396.4mm
Distance of manipulator	196mm	200mm

6. CONCLUSION

In this paper, we propose a reconstruction method of pipe shape by using an omni-directional laser and an omni-directional camera with light section method and structure from motion.

Experimental results showed the effectiveness of the proposed method.

As future work, we should install the proposed sensor to inspection robot. Also we will give texture information to measurement result which is effective to recognition of the pipe statet.

REFERENCES

1. A. Ahrary, A..A.F Nassiraei and M. Ishikawa, "A Study of Anautonomous Mobile Rrobot for a Sewer Inspection System," Journal of Artificial Life and Robotics, Vol.11, No.1, pp.23-27, 2007.
2. K.U. Scholl, V. Kepplin, K. Berns, and R. Dillmann, "Controlling a Multijoint Robot for Autonomous Sewer Inspection," Proceedings of the 2000 IEEE International Conference on Robotics and Automation (ICRA 2000), pp.1701-1706, 2000.
3. H.B. Kuntze and H. Haffner, "Experiences with the Development of a Robot for Smart Multisensoric Pipe Inspection," Proceedings of the 1998 IEEE International Conference on Robotics and Automation (ICRA 1998), pp.1773-1778, 1998.
4. A. Zagler, and F. Pfeiffer, " "MORITZ" a Pipe Crawler for Tube Junctions," Proceedings of the 2003 IEEE International Conference on Robotics and Automation (ICRA 2003), pp.2954-2959, 2003.
5. M.Horodinca, I.Doroftei and E.Mignon, "A Simple Architecture for In-Pipe Inspection Robots," Proceedings of the 2002 International Colloquium on Mobile and Autonomous Systems, (ICMAS 2002), pp.1-4, 2002.
6. K. Suzumori, S. Wakimoto and M. Tanaka, "A Miniature Inspection Robot Negotiating Pipes of Widely Varying Diameter," Proceedings of the 2003 IEEE International Conference on Robotics and Automation (ICRA 2003), pp.2735-2740, 2003.
7. J. Gaspar, N. Winters and J. S. Victor, " Vision-Based Navigation and Environmental Representations with an Omnidirectional Camera," IEEE Transactions on Robotics and Automation, Vol.16, No.6, pp.890-898, 2000.
8. Y. Yagi, " Omnidirectional Sensing and Its Applications," IEICE Transactions on Information and Systems, Vol.E82-D, No.3, pp.568-579, 1999.
9. J. Gluckman, and S. K. Nayar, "Ego-motion and Omnidirectional Cameras," Proceedings of the 6th International Conference on Computer Vision, pp.999-1005, 1998.
10. J. Kannala, S. S. Brandt, and J. Heikkilä, "Measuring and Modelling Sewer Pipes from Video," Machine Vision and Applications, Vol.19, No.2, pp.73-83, 2008.
11. A. Yamashita, H. Higuchi and T. Kaneko, "Three Dimensional Measurement of Object's Surface in Water Using the Light Stripe Projection Method," Proceedings of the 2004 IEEE International Conference on Robotics and Automation (ICRA2004), pp.2736-2741, 2004
12. Y. Yachide, Y. Oike, M. Ikeda. and K. Asada, "Real-time 3-D Measurement System Based on Lght-Section Method Using Smart Image Sensor," Proceedings of the 2005 IEEE International Conference on Image Processing (ICIP 2005), pp.III-1008-1011, 2005
13. R.B.Fisher and D.K.Naidu, "A Comparison of Algorithms for Subpixel Peak Detection," Proceedings of the 1991 British Machine Vision Association Conference (BMVAC 1991), pp.217-225, 1991.
14. R. Kawanishi, A. Yamashita and T. Kaneko, "Construction of 3D Environment Model from an Omni-Directional Image Sequence," Proceedings of the 3rd Asia International Symposium on Mechatronics (AISM 2008), TP1-3(2), pp.1-6, 2008.
15. D. G. Lowe, "Distinctive Image Features from Scale-Invariant Keypoints," International Journal of Computer Vision, Vol.60, No.2, pp.91-110, 2004.
16. M. A. Fischler and R. C. Bolles, "Random Sample Consensus: A Paradigm for Model Fitting with Applications to Image Analysis and Automated Cartography," Communications of the ACM, Vol.24, No.6, pp.381-395, 1981.
17. B. Triggs, P. McLauchlan, R. Hartley and A. Fitzgibbon, "Bundle Adjustment -A Modern Synthesis," Vision Algorithms: Theory & Practice, Springer-Verlag LNCS 1883, 2000.